Simulation of Particle Deposition in an Airplane Cabin Mockup

Miao Wang
School of Mechanical Engineering
Purdue University
West Lafayette, IN 47906, USA
wang283@purdue.edu

Chao-Hsin Lin
Environmental Control Systems
Boeing Commercial Airplanes
Everett, WA 98124, USA
chao-hsin.lin@boeing.com

Qingyan Chen
School of Mechanical Engineering
Purdue University
West Lafayette, IN 47906, USA
yanchen@purdue.edu
and
School of Environmental Science and Technology
Tianjin University
Tianjin 300072, China
yanchen@tju.edu.cn

Abstract— **Accurate prediction of particle deposition in airliner cabin is important to estimate exposure risk of occupants to infectious diseases. This investigation simulated airflow field, particle dispersion and deposition in a half-occupied four-row cabin mockup using a Detached-Eddy Simulation (DES) model with a modified Lagrangian method. Three types of particles with diameters of 0.7, 10 and 100 μm were studied that represent different particle dispersion and deposition processes. This study tested two flow scenarios: one is a breathing case in which particles were released from an index occupant with very small inertial force; and the other is a coughing case in which the particles were released by a high momentum jet flow. This study found that the DES model with the modified Lagrangian method can predict reasonably good results for air velocity, particle concentration and deposition in the cabin environment. The particle deposited depended on particle size and inertial forces. For the breathing case, the deposition rate on the cabin surfaces was 35% for the small (0.7 μm) particles, 55% for the medium (10 μm) particle and 100% for the large (100 μm) particles. In the coughing case, the particle deposition was enhanced due to the high initial velocity. The particle deposition rate was 48%, 69%, and 100% for the small, medium and large particles, respectively.**

Keywords-CFD; experiment; particle; deposition; indoor

I. INTRODUCTION

Over four billion people arrive at and depart from airports all over the world every year. This figure will double by 2025, according to a long term traffic forecast [1]. Commercial airplane passengers travel in an enclosed cabin environment at close proximity [2]. During the long time of air travel, the exposure risk to infectious diseases can be very high. Mangili and Gendreau [3] evaluated the risk of infectious disease transmission in commercial airplane cabins and concluded that air travel was an important factor in the worldwide spread of infectious diseases.

Infectious disease transmission in airplane cabins can occur in many ways, such as direct contact with contagious particles generated from an infected person, inhaling pathogenic airborne agents or droplets, or touching contaminated surfaces. These different disease transmission paths are all closely related to the deposition and transport of contaminant particles or droplets. For example, saliva droplets generated by an index person through coughing or sneezing can deposit directly on the mouth or eyes of another person. The dose of airborne infectious agents and droplets is associated with their deposition rate and transport path, and a surface in an airplane cabin can be contaminated by the trapping of contaminant particles. As the commercial airplane cabins are crowded and packed with different solid surfaces, their influence on particle deposition and transport can be significant. Therefore, it is essential to evaluate the level and distribution of particle deposition in a cabin environment.

The rapid growth of computer power makes CFD a promising tool for predicting airflows, particle transportation, and deposition in enclosed environments [4,5]. For cabin airflow and contaminant transport simulation, Baker et al. [6] validated their CFD prediction of air velocity and mass transport inside an aircraft cabin using measurement data. Zhang et al. [7] measured and simulated gaseous and particulate contaminant transport in a four-row cabin mockup. Poussou et al. [8] simulated transient flow and contaminant concentration field in a small-scale cabin mockup with a moving body. These studies explored complicated airflow and contamination concentration fields inside a cabin environment. However, particle deposition on cabin surfaces was neglected in these cases, which could be significant for a crowded cabin environment.

Particle deposition has been studied by many researchers, however, for other enclosed environments. Lai and Nazaroff [9] applied an analogous model for particle deposition to smooth indoor surfaces and predicted a reasonable result for simple geometry. Lai and Chen [10] conducted a Lagrangian simulation for aerosol particle transport and deposition in a chamber and found good agreement between their CFD

result and the empirical estimation. Zhao et al. [11] simulated particle deposition in ventilated rooms. Their deposition results agreed with the measured data at low turbulence level, but failed to match the experimental data when the turbulence was high. Zhang and Chen [12] simulated particle deposition on differently oriented surfaces inside a cavity using a modified Lagrangian method and predicted improved results. Although reasonable prediction of deposition was reported by many studies, the relatively simple geometry and airflow conditions in these cases may not guarantee a good result in a much more complex environment such as an airplane cabin. A study of the literature showed that particle deposition inside an airplane cabin has not been well investigated by either numerical or experimental studies.

Using numerical simulations, this paper aims to extend the understanding of contagious particle depositions inside an airplane cabin environment. This investigation first evaluated a modified Lagrangian particle deposition model with Detached Eddy Simulation (DES) [13] and applied it to a four-row cabin mockup. The simulation included two flow scenarios, one breathing and talking case, and the other a coughing case. The particle depositions on different cabin surfaces were determined from the simulation results. The study discussed the deposition statistics and identified key factors related to particle depositions in airplane cabins.

Section I of this paper introduces the background information of this study. Section II shows the numerical models used in the simulation. Section III shows the test case and simulation results. Section IV discusses the result. Section V concludes this study.

II. AIRFLOW AND PARTICLE PHASE MODELS

Accurate models of airflow and turbulence in an indoor environment are important for predicting the particle transportation and deposition process. This study used the DES Realizable k-ε model [13], which can provide accurate prediction of air velocity and turbulence quantities [14]. Due to limited space available, the formulation of this model was not included in this paper, but can be found from literature [13].

With the airflow information, this study modeled the particle dispersion and deposition with a Lagrangian method, which can be expressed as:

$$\frac{d\vec{u}_p}{dt} = F_D\left(\vec{u} - \vec{u}_p\right) + \frac{\vec{g}\left(\rho_p - \rho\right)}{\rho_p} + \vec{F} \qquad (1)$$

where $\vec{u}_p$ and $\vec{u}$ are the particle and air velocities, respectively; ρ_p and ρ are the densities of particles and air

respectively; $\vec{g}$ is the gravitational force; $\vec{F}$ is other forces such as the Thermophoretic force, Saffman lift force, and Brownian force; and is the drag coefficient.

In (1), the term $\vec{u}$ represents the actual airflow velocity, which should be written as:

$$\vec{u} = \bar{u} + u' \qquad (2)$$

where $\bar{u}$ is the velocity solved by the DES model, u' is the turbulence velocity component that should be properly modeled. Although there is no model available for the DES model used in this study, many models have been developed for different RANS models, which may be used by the DES in its near wall region. This study applied a deposition model proposed by Matida et al. [15].

$$u_i' = \begin{cases} \zeta_i A u^* y^{+2} & y^+ \le 4 \\ \zeta_i \sqrt{2k/3} & y^+ > 4 \end{cases} \qquad (3)$$

where $A = 0.008$ is a constant, u^* is the shear velocity, and y^+ is the distance from a particle to the nearest wall in the wall unit.

III. PREDICTION OF PARTICLE DEPOSITION IN A FOUR-ROW AIRPLANE CABIN

A. Case Description

Fig. 1 depicts the schematic of the four-row twin-aisle cabin mockup. In the experiment [7], the cabin mockup had 28 seats, 14 of which were occupied by human simulators, as shown in red in the figure. The air was supplied from two groups of linear diffusers located near the center of the ceiling. The total airflow rate was 0.23 m³/s, or 8.2 L/s per passenger seat. Three-dimensional air velocity and air temperature were measured at two planes, as depicted in green in Fig. 1. The air velocity and temperature profiles at the inlet diffuser and the temperature of different surfaces were also measured.

The particle source was located at the center seat of the third row (seat 3D), as shown in Fig. 1. Non-evaporative, monodispersed Di-Ethyl-Hexyl-Sebacat (DEHS) particles were released from the source into the cabin with a small momentum. After the airflow and particle field reached a steady-state, the particle concentration was measured at eight positions, as shown in Fig. 1. The particle used in the experiment had a diameter of 0.7μm. However, in the CFD simulation, three sizes of particles (0.7, 10, and 100μm) were simulated to study the influence of particle size on the particle deposition.

The numerical simulation was conducted based on CFD code ANSYS FLUENT (version 12.1). The study applied the DES Realizable k-ε model with the modified Lagrangian method as discussed before. The simulation used a solution from the RNG k-ε model as the initial field and calculated 10 minutes of flow time to reach the steady-state flow field. Then, the particles were continuously released from the

source into the cabin and were mixed with the cabin air. For each particle size, 1000 particles were generated every second. The case was calculated for another 15 minutes of flow time until the particle concentration field reached steady-state, which corresponded to six complete air changes in the cabin. The averaged air velocity, particle concentration, and deposition results were obtained in the next five minutes of flow time.
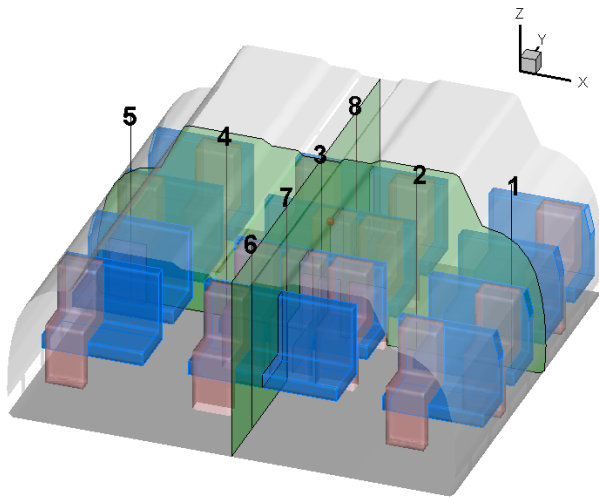
B. Air Velocity Field

Fig. 2 compares the simulated and measured air velocity vectors at the cross-section through the third row and at the mid-section along the longitudinal direction. In the cross-sectional view (Fig. 2 (a)), the ceiling diffusers and the thermal plume in the middle generated two large circulations at each side of the cabin. The prediction agreed with the measurement in terms of circulation pattern. But significant discrepancies can be found in a quantitative comparison. Similar results were also reported by Zhang et al. [7], who concluded that the simulation was very sensitive to the accuracy of the boundary conditions, which may not have been accurately measured. Note that the airflow field was asymmetrical due to the inlet and wall-boundary conditions.

In the mid-section along the longitudinal direction, the vector field shows an upward motion due to the two circulations and the thermal plume in the middle of the cabin. The CFD result agreed reasonably well with the measured data as shown in Fig. 2 (b), though differences can be found at some positions. For example, at the third row, the CFD model predicted a backward airflow motion, which was not supported by the measurements. At the same location, the CFD results also predicted a smaller upward velocity than did the experiment.

C. Particle Deposition onto Different Surfaces

1) Breathing and Talking

In the experiment, the particles were released with a very small initial velocity, which could be representative of the particle release from the breathing or talking of a passenger. The distribution of the particle deposition at solid walls and exhaust vents was also calculated for five minutes of flow time in this investigation. The density of the deposition was calculated as:

$$\overline{C} = \frac{N_{dA}}{N_{total} dA} \tag{4}$$

where N_{dA} was the number of particles deposited on surface area, dA, during a certain amount of time; N_{total} was the total number of particles generated during the same time; and dA was a small surface area, which was the same as the computational mesh.

Fig. 3 shows the normalized particle deposition density of the 0.7, 10, and 100 μm particles. Due to the asymmetrical airflow pattern, the deposition was also asymmetrical. For the small (0.7 μm) particles, a high particle deposition density was observed at the ceiling and side walls along the

Figure 2.   Schematic of the four-row cabin mockup [7].
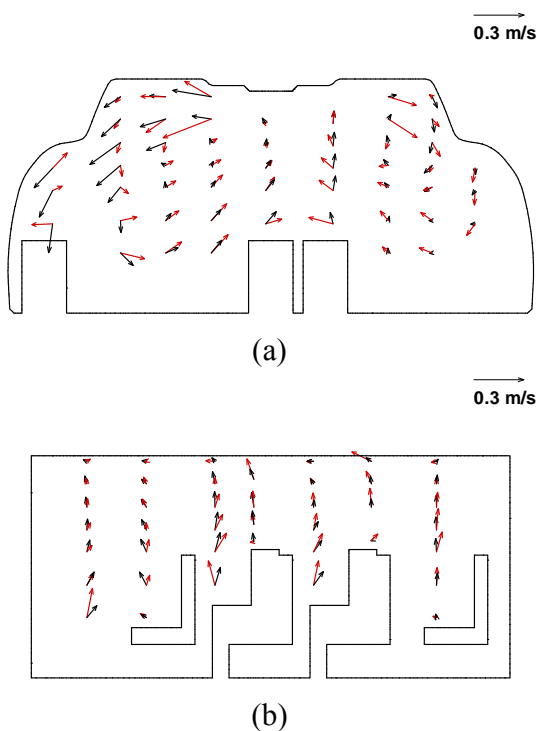
0.3 m/s

(a)

0.3 m/s

(b)

Figure 1.   Comparison of simulated (black vectors) and measured (red vectors) airflow field at: (a) the cross-section through the third row, and (b) the mid-section along the longitudinal direction.

path of the major circulation (Fig. 3(a)), while the floor and seat had relatively low deposition density (Fig. 3(d)). This is because the particles were small, and mainly followed the airflow pattern. The small 0.7 µm particles were carried by the thermal plume to reach the ceiling, where most particles joined the airflow circulation formed by the supply jets. The particles deposited at the ceiling and side walls along their path to the exhaust.

For the medium (10 µm) particles, Fig. 3(b) shows that their deposition at the ceiling and side walls was similar to that of the small particles, but the deposition rate was much lower. The deposition density at the floor was higher. As the particle size increased, the gravitational force became comparable to the drag force, which changed the deposition distribution.

For the large (100 µm) particles, Fig. 3(c) shows no

TABLE I.   STATISTICS OF PARTICLE DEPOSITION ON DIFFERENT TYPES OF SURFACES

Surfaces	Deposition Percentage					
	Breathing and talking			Coughing		
	0.7 µm	*10 µm*	*100 µm*	*0.7 µm*	*10 µm*	*100 µm*
Exhaust	65%	55%	0	52%	31%	0
Passenger	7%	8%	100%	20%	14%	2%
Floor	3%	21%	0	15%	49%	91%
Ceiling	8%	2%	0	4%	1%	0
Side wall	12%	10%	0	4%	1%	0
Section end	2%	1%	0	2%	1%	0
Seat back	1%	1%	0	1%	1%	4%
Seat front	1%	1%	0	1%	1%	0
Tray table	1%	1%	0	1%	1%	3%

deposition on the ceiling and side walls. All the particles were deposited at the surfaces of passenger 3D, as shown in Fig. 3(f). For particles of this size, the gravitational force was dominant. The particles had a free fall motion from its source (mouth/nose) and deposited within a very small area on passenger 3D.

2) Coughing

This study further modified the initial conditions for the particles so as to study the particle deposition with a cough from a passenger. The inlet velocity, flow rate, area of opening, and angle of the jet flow from the cough were chosen according to Gupta et al. [16]. As in the previous case, seven sizes of particles were continuously released from the cough by the passenger at seat 3D. All the models and simulation procedures were the same as in the breathing and talking case.

Fig. 4(a) shows the normalized particle deposition density of the 0.7 µm particles at the ceiling and side walls. Compared with the previous case, the deposition on the ceiling and side walls was significantly reduced. This was because the jet flow that carried the particles could penetrate the thermal plume. Therefore, most of the particles did not enter the major circulation so they could not reach the ceiling. For the deposition on the floor and seats, Fig. 4(d) shows a high deposition density on the seat back of passenger 2D, the surface of passenger 3D, and the floor area close to seat 3D, due to the jet impingement.

For the 10 µm particles, Fig. 4(b) shows a lower deposition density at the ceiling and side walls than that for

the breathing and talking case. As shown in Fig. 4(e), a high deposition density was observed in the areas of jet impingement. Unlike the 0.7 µm particles that mostly suspended in the air after entering the air, a majority of the 10 µm particles deposited due to the jet momentum and the gravity.

For the 100 µm particles, Fig. 4(c) shows that no particles deposited on the ceiling and side walls. All the particles deposited on the back surface of seat 2D, the surface of passenger 3D, and the floor close to seat 3D due to direct impingement and gravity because these particles were too heavy to be carried by the airflow.

IV.   DISCUSSION

Table I shows the statistics of the particle deposition on different types of surfaces. For the breathing and talking case, 65% of the 0.7 µm particles were removed by air through the exhaust. The side walls and ceiling trapped a large portion of the particles (12% and 8%, respectively). These surfaces may not be frequently contacted by passengers. The passenger surfaces had 7% of the 0.7 µm particles. Despite the large area, the floor only received 3% of the particles. The two section ends trapped 2% of the particles because the airflow along the longitudinal direction was small. The seat front, seat back, and tray tables trapped 3% of the particles that could likely be touched by the passengers. For the 10 µm particles, the number of particles exhausted was reduced to 55%, but was still a majority. The deposition on the ceiling decreased to 2% since gravity became important for this size of particle. For the 100 µm particles, all the particles deposited on the surface of the index passenger, which can be explained by their free fall motion. In general, the gravity force played a major role in the particle deposition.

In the coughing case, the jet could penetrate the thermal plumes and could transport the particles to the lower part of the cabin. The jet impingement enhanced particle deposition on the floor, thus increasing the total particle deposition by 13% and 14% for the 0.7 µm and the 10 µm particles, respectively. For the two particle sizes, the deposition on the passenger also increased. The deposition on the ceiling and side walls decreased slightly. About 91% of the 100 µm particles deposited on the floor, with the rest on the seat back and tray table in front of the index passenger.

V.   CONCLUSION

This study applied the DES model with a modified Lagrangian method to predict the particle dispersion in a four-row airplane cabin mockup. By comparing with the experimental data, this investigation found that this new model can predict reasonably good results for air velocity, particle concentration, and particle deposition.

For the cabin case, three sizes of particles were assumed to be released by an index passenger sitting in the middle of the cabin due to breathing with zero velocity and due to coughing with suitable jet velocity. This study found that the distribution of particle deposition onto surfaces depended on particle size, particle release mode, and the airflow pattern in

the cabin. In the breathing case, 35% of the small (0.7μm) particles, 55% of the medium (10μm) particles, and 100% of the large (100μm) particles deposited onto the cabin surface and the rest were removed by the cabin ventilation. In the coughing case, the number of small, medium and large particles deposited changed to 48%, 69%, and 100%, respectively.

REFERENCES

[1] ACI. The Global Airport Community, 2007. www.airports.org/aci/aci/file/Annual Report/ACI Annual Report 2006 FINAL.pdf . Last accessed 09/17/2011.

[2] J. D. Spengler and D. G.Wilson, "Air Quality in Aircraft," Proceedings of the Institution of Mechanical Engineers, Part E: Journal of Process Mechanical Engineering 217, 2003, pp. 323-335.

[3] A. Mangili and M.A.Gendreau, "Transmission of infectious diseases during commercial air travel," Lancet 365, 2005, pp. 989-996.

[4] P. R. Spalart and D. R. Bogue, "The role of CFD in aerodynamics, off-design," Aeronautical Journal 107(1072), 2003, pp. 323-329.

[5] Q. Chen, "Ventilation performance prediction for buildings: A method overview and recent applications," Building and Environment 44(4), 2008, pp. 848-58.

[6] A. J. Baker, S. C. Ericson J.A. Orzechowski, K.L. Wong and R. P. Garner, "Aircraft passenger cabin ECS-generated ventilation velocity and mass transport CFD simulation: Mass transport validation exercise," Journal of the IEST (Online) 51(1), 2008, pp. 90-113.

[7] Z. Zhang, X. Chen, S. Mazumdar, T. Zhang and Q. Chen, "Experimental and numerical investigation of airflow and contaminant transport in an airliner cabin mockup," Building and Environment 44(1), 2009, pp. 85-94.

[8] S. Poussou, S. Mazumdar, M. W. Plesniak, P. Sojka and Q. Chen, "Flow and contaminant transport in an airliner cabin induced by a moving body: Scale model experiments and CFD predictions," Atmospheric Environment 44(24), 2010, pp. 2830-2839.

[9] A. C. K. Lai and W. W. Nazaroff, "Modeling indoor particle deposition from turbulent flow onto smooth surfaces," Journal of Aerosol Science 31, 2000, pp. 463-476.

[10] A. C. K. Lai and F. Chen, "Modeling of particle deposition and distribution in a chamber with a two-equation Reynolds-averaged Navier–Stokes model," Journal of Aerosol Science 37(12), 2006, pp. 1770-1780.

[11] B. Zhao, C. Yang, X. Yang and S. Liu, "Particle dispersion and deposition in ventilated rooms: Testing and evaluation of different Eulerian and Lagrangian models," Building and Environment 43(4), 2008, pp. 388-397.

[12] Z. Zhang and Q. Chen, "Prediction of particle deposition onto indoor surfaces by CFD with a modified Lagrangian method," Atmospheric Environment 43(2), 2009, pp. 319-328.

[13] FLUENT, 2005. Fluent 6.2 Documentation. Fluent Inc., Lebanon, NH.

[14] M. Wang, and Q. Chen, "Assessment of various turbulence models for transitional flows in enclosed environment," HVAC&R Research 15(6), 2009, pp. 1099-1119.

[15] E. A. Matida, W. H. Finlay, C. F. Lange and B. Grgic, "Improved numerical simulation of aerosol deposition in an idealized mouth–throat," Journal of Aerosol Science 35, 2004, pp. 1-19.

[16] J. K. Gupta, C.-H. Lin, and Q. Chen, "Flow dynamics and characterization of a cough," Indoor Air 19, 2009, pp. 517-525.
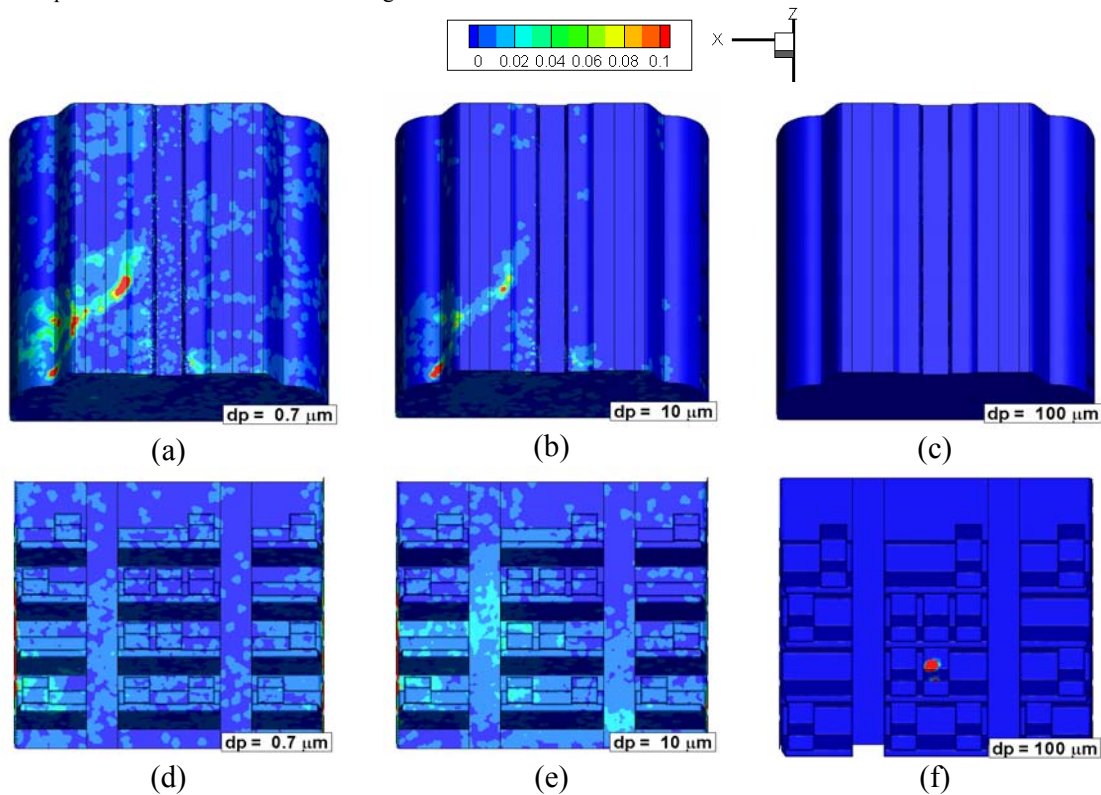
Figure 3. Particle depositions at different surfaces for the breathing and talking case: the top row is for the ceiling and side wall surfaces and the bottom row for the floor and seats surfaces (a) and (d) for 0.7 μm particles, (b) and (e) for 10 μm particles, and (c) and (f) for 100 μm particles.
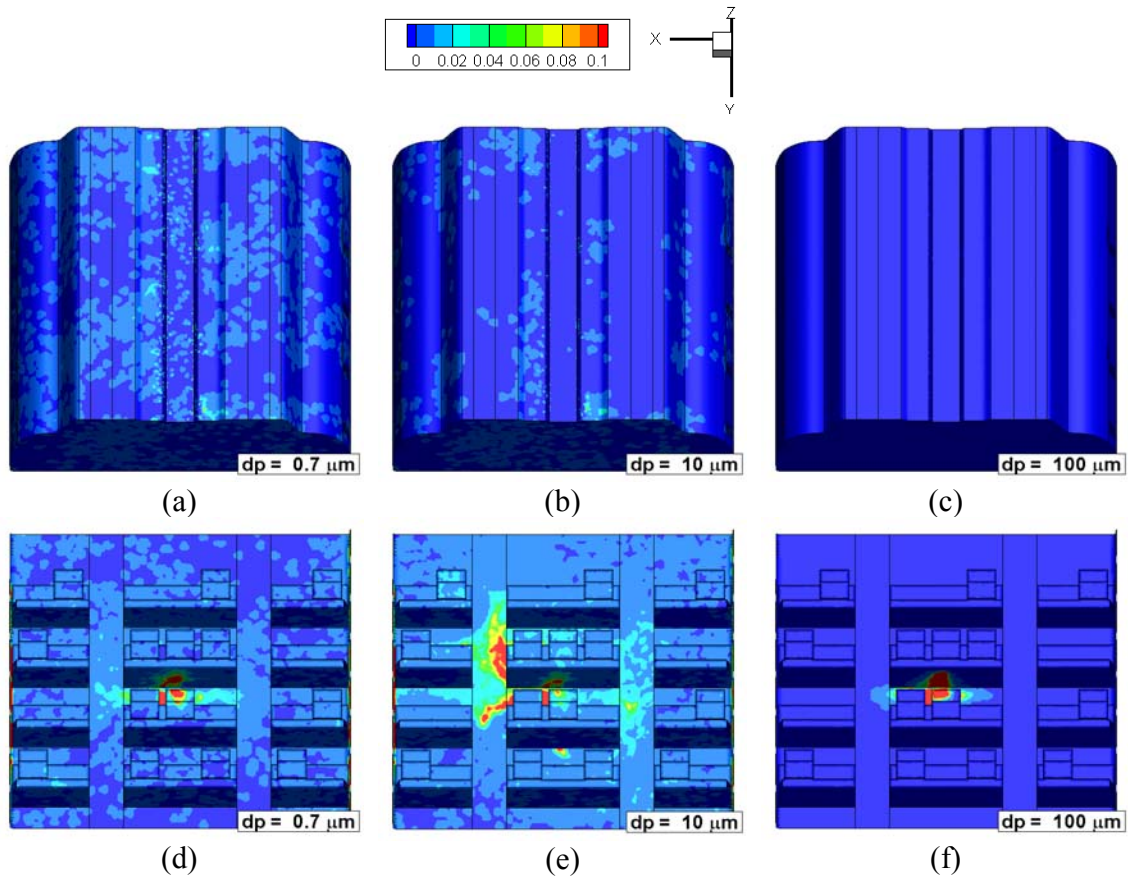
Figure 4.   Particle depositions at different surfaces for the coughing case: the top row is for the ceiling and side wall surfaces and the bottom row is for the floor and seats surfaces (a) and (d) for 0.7 μm particles, (b) and (e) for 10 μm particles, and (c) and (f) for 100 μm particles.